Nondestructive Evaluation for Yield Strength and Toughness of Steel Pipelines

S. D. Palkovic[1,2], K. Taniguchi[1], S. C. Bellemare[1,2]

1: Massachusetts Materials Technologies, LLC, Cambridge, MA
2: Massachusetts Institute of Technology, Cambridge, MA

Correspondence: Steven Palkovic – (617) 502-5636; s.palkovic@bymmt.com

Material mechanical property data including fracture toughness help address potential integrity threats such as material loss through corrosion, stress corrosion cracking (SCC), and fatigue. In-the-ditch (ITD) nondestructive evaluation (NDE) of mechanical properties has expanded beyond traditional hardness testing to provide measurements of strength and fracture toughness of metals without the need for sample removal and laboratory testing. This paper describes two new and complementary mechanical testing methods recently applied to vintage pipeline steels as input to integrity management. In the first method, hard blunt styluses of different geometries slide over the pipe surface at constant loads to measure material hardness. The hardness values for dissimilar styluses are input into predictive equations to determine the yield strength and ultimate tensile strength of the steel. When performed over longitudinal seams or girth welds, the tests identify the heat treatment including normalization. In the second method, the instrument is equipped with a wedged-shaped stylus that includes an opening, or stretch passage, where material is locally subjected to tension that results in microvoid growth and coalescence that match laboratory ductile fracture. The material response is correlated with the fracture toughness through measuring the crack tip opening displacement. Field studies and validation provide examples of application of the methods.

1 Introduction

The United States relies on 300,000 miles of high pressure pipelines to transmit oil and natural gas across the country [1]. This infrastructure is maintained through integrity management programs that utilize data from both in-line-inspection (ILI) and in-the-ditch nondestructive evaluation (NDE) technologies. Whereas ILI devices are capable of testing long sections of pipelines to group populations of pipe joints exhibiting similar characteristics, NDE technologies provide precise measurements of mechanical properties to support engineering critical assessment. Through further validation and standardization, these direct assessment programs may provide alternatives to more costly and invasive procedures such as material sampling through hot taps or hydrostatic testing of entire line segments.

For measurement of tensile strength properties, there have been a number of advancements since the implementation of Brinell hardness which was first approved as a testing standard by the American Society for Testing and Materials (ASTM) in 1924 [2]. One improvement is Instrumented Indentation Testing (IIT) that was originally proposed by Haggag et al. and uses a spherical stylus subjected to a series of indentations with increasing loads to measure the flow strength of the material with increasing strain [3]. This approach requires a material-dependent empirical factor to account for friction and material deformation around the stylus. More recently, a numerical approach based on finite element analysis simulations of load-indentation curves was proposed by Dao et al. for materials exhibiting a power-law strain hardening behavior [4]. The authors found that the accuracy of the technique for measuring tensile properties was greatly improved by using two styluses with dissimilar geometries to test the material at different representative strains [5]. Despite the lack of empirical factors, a major shortcoming was the high sensitivity to measurement error during testing.

Unlike strength properties, fracture toughness describes a material's ability to resist the growth of a crack and allows for the calculation of the maximum allowable flaw size. This is particularly important for corrosive environments like oil and gas pipelines where the pipeline material is susceptible to embrittlement and stress corrosion cracking (SCC). The existing methods for NDE fracture toughness measurement have been limited to indentation tests that are analyzed according to an empirical critical fracture strain model [3]. Widespread application of this method is challenging because it induces a plastic deformation in the material that is not indicative of fracture processes in metallic materials.

Massachusetts Materials Technologies (MMT) has recently developed novel NDE methods for characterization of both tensile and fracture properties. Both methods are based on frictional sliding where a stylus is indented into the material surface, and then slides along the surface to create a permanent groove. For tensile properties, the Hardness Strength and Ductility (HSD) Tester utilizes dissimilar stylus geometries to induce varying magnitudes of plastic deformation in the material. The measured response at each stylus is used to construct a complete stress-strain curve that defines the material behavior from initial yield to the ultimate tensile strength (UTS). Fracture toughness is measured with the Nondestructive Toughness Tester (NDTT), which uses a specially designed wedge-shaped stylus to induce microvoid growth and coalescence within a small ligament of surface material.

This paper details the development and validation of both the HSD and NDTT. Section 2 describes HSD Tester methodology, and provides comparison of HSD yield strength measurements with laboratory tensile tests for homogeneous steel plates and seam-welded pipes. A unique application of the HSD Tester to characterize the fabrication methods for electric resistance welded (ERW) and flash welded pipes is provided in Section 2.3. In Section 3 the mechanics of the NDTT are defined, with initial proof-of-concepts performed on a steel and aluminum alloy.

2 Hardness Strength and Ductility (HSD Tester)

2.1 Fundamentals of Frictional Sliding for Tensile Properties

A frictional sliding test is demonstrated in Figure 1, where a hard stylus is indented into a softer material and then slides along the surface to create a permanent residual groove. The correlation between frictional sliding and tensile testing was first defined by Bellemare et al. who used finite element analysis (FEA) models to calculate the elastic-plastic response of power-law hardening materials with a conical stylus [6-8]. This work illustrated that the normal load on the stylus and the dimensions of the residual groove profile that remains in the material define a unique solution for the tensile strength properties [8]. Furthermore, compared to indentation techniques, frictional sliding allows for a larger number of measurements along the length of the groove which can be averaged to reduce the test sensitivity.

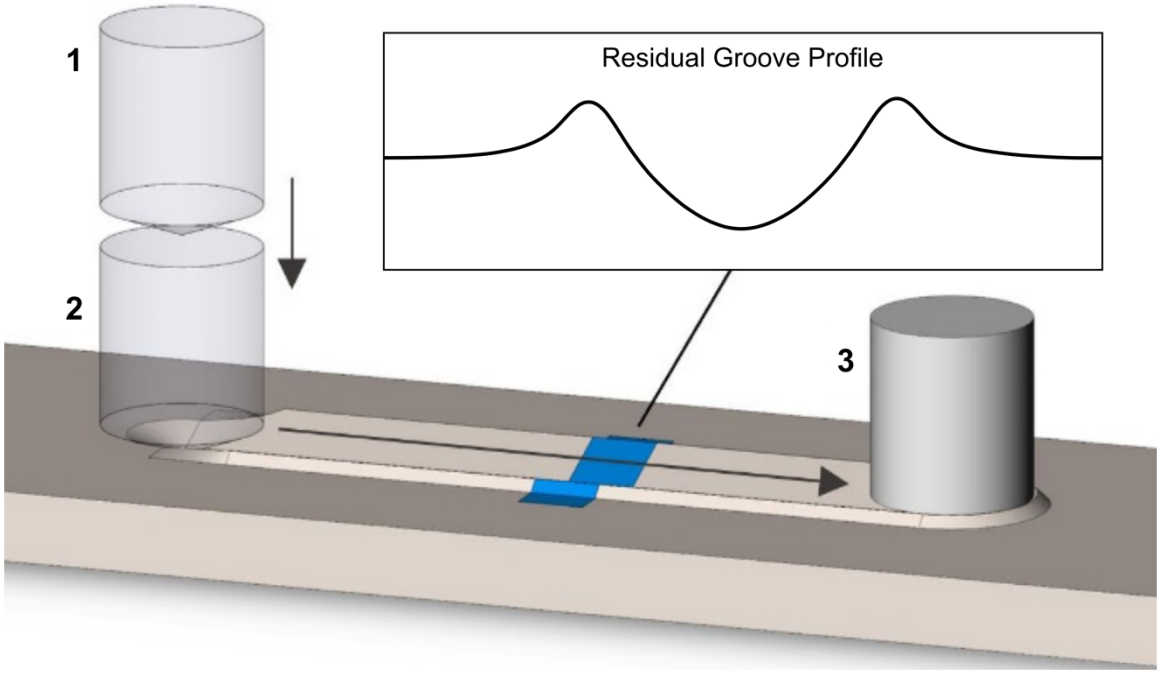

Figure 1: A frictional sliding experiment consists of (1) a hard stylus that is (2) indented into the surface of a softer material and (3) slides along the surface to form a permanent groove. For a given stylus geometry and contact condition, the residual groove profile is a unique function of the material elastic-plastic properties [8].

The HSD Tester is the first commercial implementation of the frictional sliding methodology for NDE measurement of tensile properties. This device extends the Bellemare et al. frictional sliding methodology to multiple styluses to provide greater accuracy and reliability. Data collected from an HSD experiment is analyzed using predictive functions that are based on FEA simulations of

the frictional sliding process for a range of stylus geometries and contact conditions. A stylus with a larger radius and shallower penetration induces less overall strain in the material to measure the material response near the yield point, whereas a smaller radius and greater penetration depth results in a higher strain magnitude near the ultimate tensile strength (UTS). This concept is illustrated by the plastic strain distributions and representative stress-strain equations shown in Figure 2. A complete stress-strain curve is obtained by fitting a power-law to the four independent stylus measurements. The current predictive functions are entirely based on the numerical solution of the three-dimensional contact mechanics problem that has been obtained through over 300 FEA simulations of a large combination of material properties, and requires no empirical factors or assumptions on deformation behavior. This database of material inputs covers the full range of steel stress-strain properties.

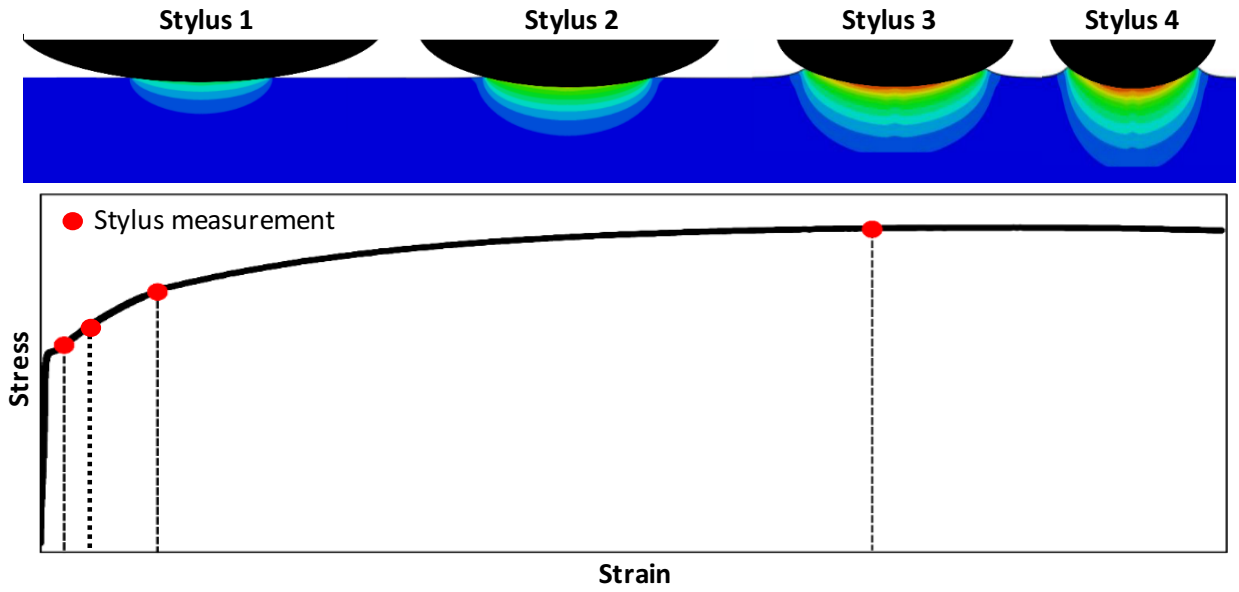

Figure 2: The HSD prediction method uses dissimilar stylus geometries to probe the material response at varying stress-strain values, allowing for the prediction of the complete stress-strain response based on the individual measurements at each stylus.

The HSD technology has been validated by testing homogeneous steel samples with the HSD Tester and comparing the with the yield strength predicted through destructive laboratory tensile tests. Table 1 shows the results of validation testing for the 0.5% elongation under load (EUL) yield strength prediction for 15 different steel materials, and finds excellent agreement between the two methods with the absolute value of the average error being approximately 3.3%. This difference does not account for the intrinsic variability of laboratory tensile testing. ASTM E8-09, Section 9 – Precision and Bias, states that the repeatability coefficient of variation between laboratories in yield strength determination in accordance with ASTM E8 was as high as 4.5% [9]. This suggests that the HSD Tester is comparable to tensile tests for homogeneous materials.

Table 1: Validation of yield strength prediction for homogeneous steel materials.

Sample	Tensile 0.5% EUL Yield Strength		HSD 0.5% EUL Yield Strength		Difference
	(ksi)	(MPa)	(ksi)	(MPa)	(%)
08T2	37.0	255	37.0	255	0.0
F004	43.4	299	41.0	283	-5.9
24T2	44.0	303	46.2	319	4.8
12SLF	45.5	314	46.0	317	1.1
14GRB	47.3	326	49.4	341	4.3
12Y64	50.3	347	51.1	352	1.6
18GRB-B	52.2	360	51.8	357	-0.8
F001	53.8	371	54.6	377	1.5
16X42	55.7	384	57.5	397	3.1
F015	56.5	390	59.1	408	4.4
10SHF	65.0	448	61.9	427	-5.0
16GRB	70.0	483	71.0	490	1.4
16X52	70.8	488	64.9	448	-9.1
F005	71.7	494	70.1	483	-2.3
T3011	72.7	501	69.8	481	-4.2

2.2 **Application of the HSD Tester for Transmission Pipelines**

The HSD Tester is a portable device that can perform measurements on an exposed pipe, fitting, or other metal component. Prior to testing, a 3x4 in. area of material is polished using a 10-minute surface preparation procedure. Figure 3(a) shows the HSD Tester attached to the outer diameter of a transmission pipeline during an integrity dig. The four grooves generated during testing are less than 0.002 inches (50 microns) deep and are shown in Figure 3(b). The unit consists of an enclosure that protects internal mechanical components during field operation and maintains a clean testing surface during testing.

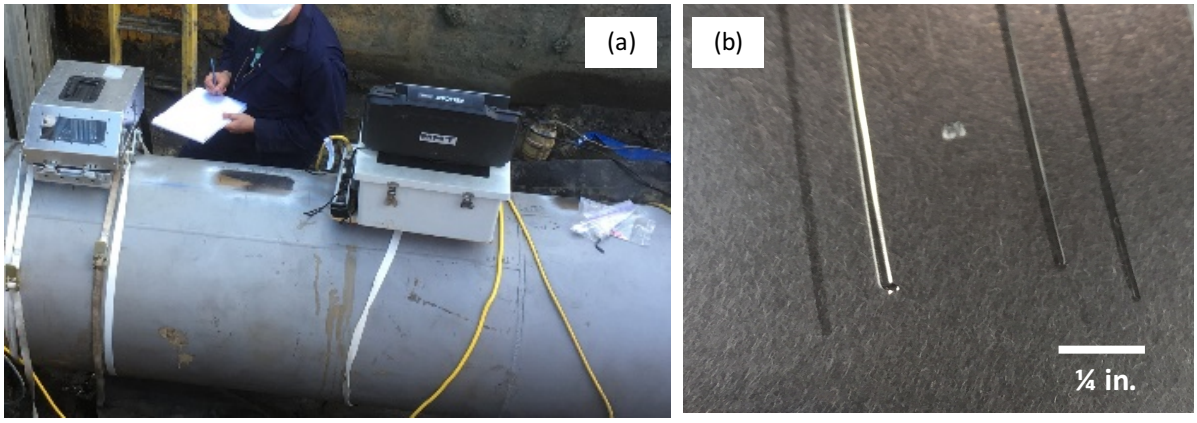

Figure 3: (a) HSD Tester operating on a transmission pipeline during an integrity assessment dig. (b) Set of four superficial grooves that remain on the surface of the pipe after a test is performed.

Seam-welded pipelines are typically not homogeneous materials. These materials have been manufactured by cold-forming a flat plate to a cylindrical pipe with a longitudinal welded. This results in a gradient in material properties through the thickness of the pipe wall, and a higher strength for an outer surface test that has experienced more strain hardening than the midwall of the pipe that remains predominantly elastic. However, additional fabrication processes such as pipe expansion or full body normalization will reduce these differences. These concepts have been previously confirmed through elastic-plastic FEA models of the pipe forming process and the

comparison of HSD tests that were performed on the outer diameter and pipe midwall [10]. A surface-to-bulk correction is applied to account for the difference between outer surface HSD measurements and tensile tests, where the bulk value is associated with the API tensile test of a full-wall thickness specimen. This correction accounts for the pipe geometry to calculate the extent of strain hardening on the outer surface. The justification for applying a surface-to-bulk correction on seam-welded pipes is based on an additional HSD test performed across the longitudinal welded seams. This is discussed in greater detail in Section 2.3. Applying this procedure, the results for yield strength prediction of 16 different steel materials and the corresponding full-wall thickness tensile tests are shown in Table 2 [11]. The absolute value of the average error for pipe samples is approximately 4.0%.

Table 2: Validation of yield strength prediction for seam-welded pipe materials. HSD experiments were performed on the outer surface of pipe specimens, and tensile test were full-wall thickness specimens

Sample	Tensile 0.5% EUL Yield Strength		HSD 0.5% EUL Yield Strength		Difference
	(ksi)	(MPa)	(ksi)	(MPa)	(%)
12SLF	45.5	314	47.4	327	4.0
14GRB	47.3	326	47.1	325	-0.4
22SLF	49.8	343	47.4	327	-5.1
12Y64	50.3	347	48.7	336	-3.3
16SLF	52.6	363	53.7	370	2.0
16X42	55.7	384	55.3	381	-0.7
08SHF-2	57.1	394	56.4	389	-1.2
08SHF-1	64.6	446	68.9	475	6.2
16GRB	70	483	63.3	437	-10.6
16X52	70.8	488	74.3	512	4.7
22SLF-2	49.1	339	52.3	361	6.1
16Y69-1	57.8	399	61.8	426	6.5
19Y72-1	63.1	435	64.1	442	1.6
20Y68-1	53.5	369	51.1	352	-4.7
26Y52-1	58.5	403	55.5	383	-5.4
20X42-1	58.8	406	60	414	2.0

2.3 **Longitudinal Seam Characterization**

A unique capability of the HSD tester is to continuously measure the material response as the test is performed. As shown in Figure 4, the HSD Tester uses a contact profilometer that follows behind the styluses to collect measurements of the four groove profiles. This provides material response measurements with sub-millimeter spatial resolution, allowing for the classification of weld type and identification of heat treatments for normalization.

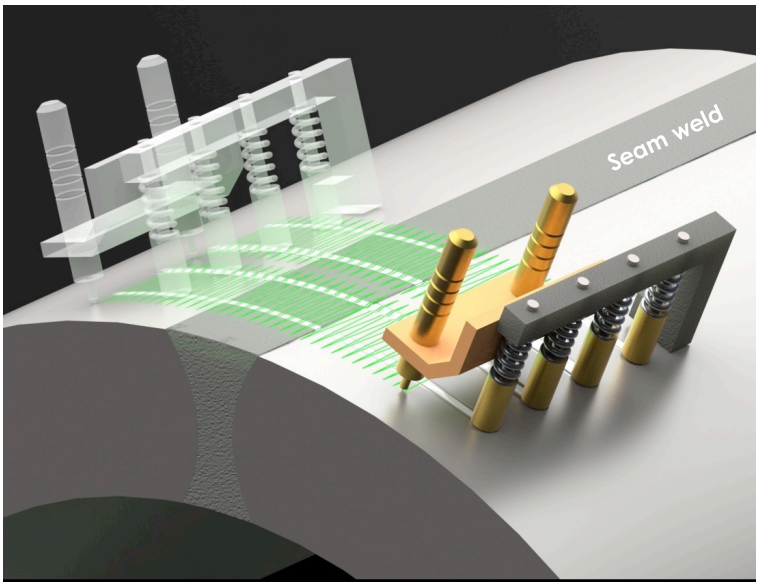

Figure 4: Overview of the HSD tester operation across a welded seam. Four independent styluses engage with the sample surface to generate permanent grooves, that are subsequently measured using a contact profilometer that rasters across the groves.

Figure 5 shows raw data collected from testing longitudinal seams of six different pipes. For Low Frequency (LF) Electro-Resistance Welded (ERW) seams Figure 5a, the increase in hardness is over a distance that spans across the two heat-affected zones without a sharp peak at the bond-line in the middle of the seam. For the High Frequency (HF) ERW seam shown in Figure 5b, there is a significant spike in hardness at the bond-line. A HF ERW seam that has been normalized results in a reduced hardness within the seam compared to the surrounding material as shown in Figure 5c. These seam tests have also been used to characterize the degree of normalization through heat treatment, and identification of Electro-Flash Welded (EFW) and Double Submerged Arc Welds (DSAW). In all cases, one or more characteristic features of the hardness profiles allow to establish a distinction. This local material strength information can indicate locations that are susceptible to reduced fracture toughness. For example, section 192.112 of the Code of Federal Regulations (CFR) “Additional Design Requirements for Steel Pipe Using Alternative Maximum Allowable Operating Pressure” refers to assuring a maximum hardness at the longitudinal seams of 280 Vickers through hardness test method HV10 or equivalent [12]. With additional testing and calibration, this technique could be made available for differentiating longitudinal seams by refined categories of toughness.

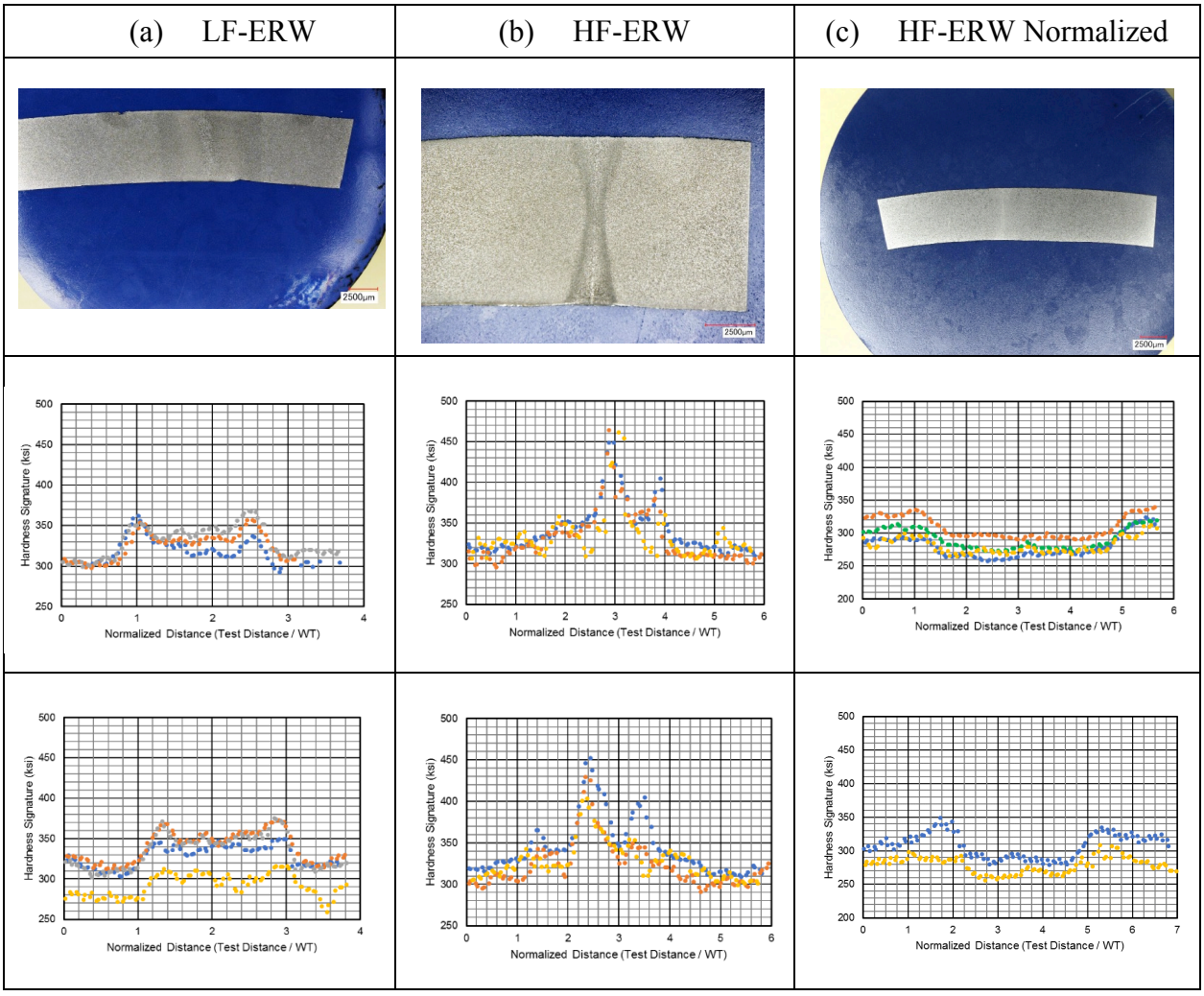

Figure 5: Hardness profiles measured during circumferential tests across the longitudinal welded seam of (a) LF-ERW pipes, (b) HF-ERW pipes, and (c) normalized HF-ERW pipes.

2.4 Field Validation Programs for the HSD Tester

The HSD Tester has been successfully used in the field to collect data for both liquid and gas transmission pipelines. Examples include the verification of material data for incomplete construction records, and strength measurement of 14 sets of pipe joints that were identified as equivalent materials through ILI tools to generate an accurate database for the entire line segment. Another project considered the evaluation of longitudinal ERW seams to determine whether they were heat-treated after welding.

3 NDE Measurement of Fracture Toughness and Bond Strength

3.1 Fundamentals of Frictional Sliding for Fracture Toughness

The Nondestructive Toughness Tester (NDTT) performs a frictional sliding test with a specially designed wedge-shaped stylus to provide an index of ductility and toughness. An overview of the NDTT mechanics is shown in Figure 6. The NDTT stylus is a traditional machining tool with an

opening that is included along the upstream face. This opening is called the stretch passage, because material that enters this region is subjected to predominantly tensile stretch. During a contact mechanics experiment, the NDTT stylus forces substrate material to flow along the upstream-face of the cutting tool, resulting in a chip that separates from the material. However, material near the stretch passage is not machined and flows through the stretch passage where it is loaded in tension until fracture. After failure, a residual ligament remains on both the cut surface of the substrate and the opposing face of the separated chip that preserves features of microvoids that formed during the ductile fracture process. A larger ligament height is indicative of a greater crack tip opening displacement which can be correlated with the fracture toughness of the material.

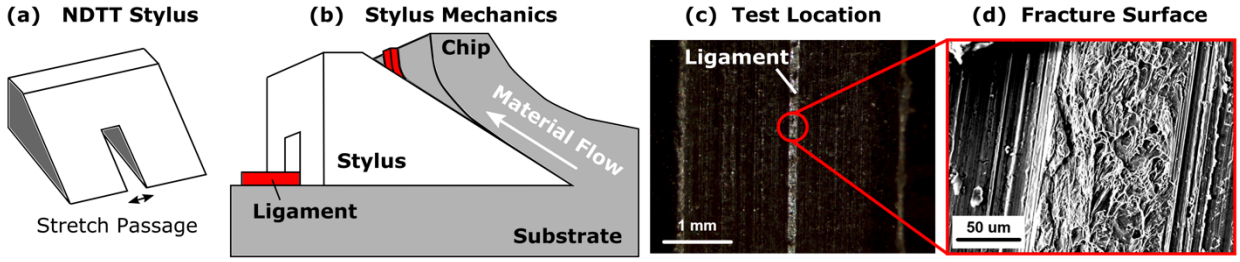

Figure 6: An overview of the NDTT stylus and mechanics. (a) The NDTT stylus utilizes a stretch passage within a traditional cutting tool. (b) Material is forced to flow up the inclined face of the stylus, resulting in a chip that separates from the substrate through a machining process. However, material contained within the stretch passage is subjected to a tensile stretch that results in a Mode-I opening fracture process. (c) The fracture surface is preserved on a ligament that remains on both the cut surface and opposing face of the chip that has separated from the substrate. (d) Fracture surface on the ligament observed with SEM

MMT performed NDTT experiments on 6061-T6 aluminum and 1020 steel materials. The test results are shown in Figure 7. A scanning electron microscopy (SEM) image of the fracture surface on the residual ligament provides clear evidence of void growth and coalescence that are signatures of tensile fracture in ductile metals. Experiments were conducted using a modified milling machine using a lathe tool with a machined stretch passage for the NDTT stylus. MMT is seeking additional support and collaboration to accelerate the research and development of NDTT technology.

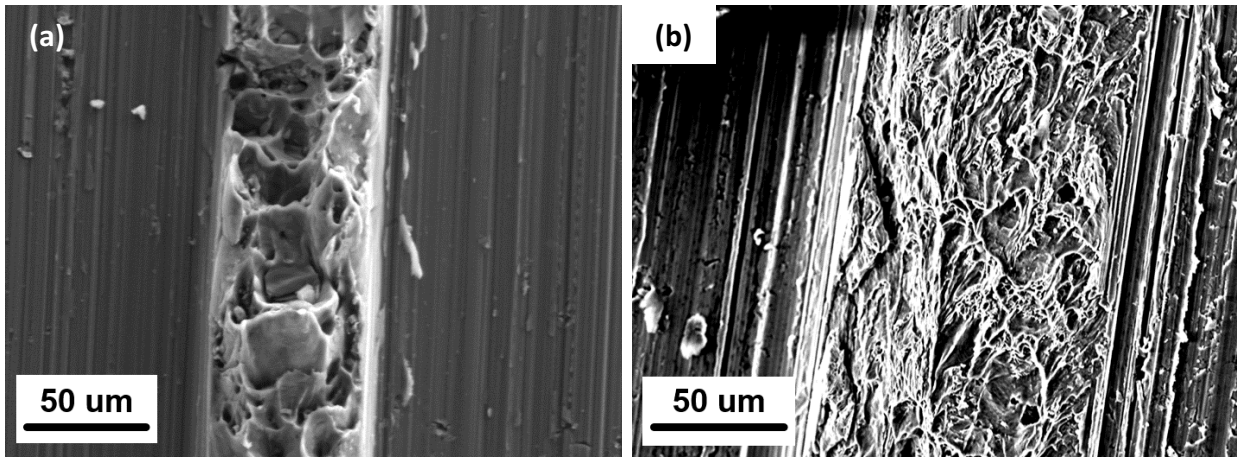

Figure 7: (a) SEM image of the fracture surface on a 6061-T6 aluminum alloy. The residual ligament that forms within the stretch passage runs vertically along the center of the image, and is surrounded by the smooth machined surface produced through the traditional cutting tool geometry. (b) A 1020 steel specimen was tested with a cut depth of 125 microns and stretch passage width of 50 microns.

3.2 Numerical Investigation of NDTT Stress-Field

A finite element analysis (FEA) model was used to study the location of the crack-tip with respect to the NDTT surface and the stress field within the stretch passage. Simulations are performed with Abaqus/Explicit using a model for damage initiation that considers ductile failure due to nucleation, growth and coalescence of voids, and shear failure due to cracks within shear bands [13]. The material model is based on an aluminum alloy EN AW-7108 TB that has been developed through experiments and validated through prior implementations with Abaqus [14]. Progressive damage is captured by the degradation of the material stiffness until failure using a linear softening relationship and a total fracture energy of 10 J/m^2. The material plasticity model follows a power-law relationship with a yield stress of 320 MPa and strain hardening exponent of 0.20. An elastic Young's modulus of 70 GPa and Poisson's ratio of 0.33 is used for elastic behavior of the aluminum alloy.

The NDTT stylus requires a three-dimensional model to capture the interaction of the FTT stylus and the substrate. The overall model is 2 mm long in the direction of cutting, 0.5 mm long in the direction of the cut-depth, and 0.55 mm wide. The model uses a stretch passage width of 50 microns and a cut-depth of 150 microns. A cutting velocity is 0.05 mm/s is used which can be considered as quasi-static. Figure 8 shows the FEA model captures the essential features observed through NDTT experiments. The ligament height is strongly dependent on the yield strength, strain hardening exponent, and fracture toughness of the simulated material. The ligament is raised above the cut surface because of the tensile stretch and deformation occurring within the stretch passage.

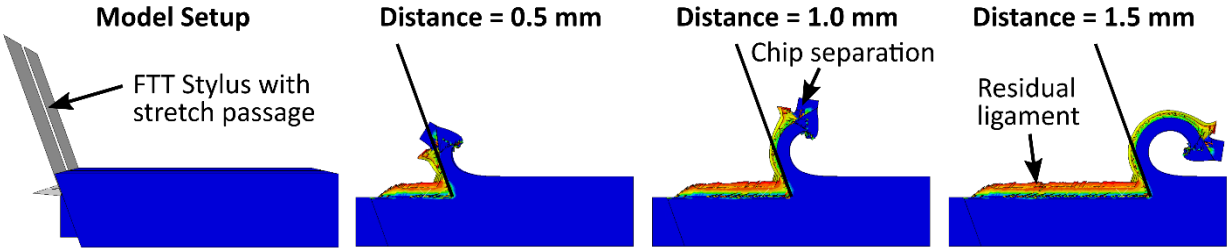

Fig. 8: Three-dimensional FEA model of fracture processes using a continuum-damage model for a ductile aluminum alloy. Elements are colored by their scalar damage index. The height of the residual ligament remaining on the cut surface is dependent on the fracture and plastic properties of the material.

Figure 9(A) shows the maximum absolute principal stress distribution within the substrate. From this image, it is clear that the crack-tip exists behind the leading face of the NDTT stylus and above the cut surface, within a region of significant tensile stress. Figure 9(B) shows the evolution of the von Mises equivalent stress and hydrostatic stress which averages all three prinicpal stress components. These values are for a representative element within the stretch passage that is loaded to failure during the simulation. When the element is ahead of the NDTT stylus, the von Mises stress begins to increase and the hydrostatic stress becomes highly compressive. However, when the NDTT stylus passes in front of the element, the hydrostatic stresses switches to significant hydrostatic tension. A larger magnitude of triaxial tension is consistent with transitions from plane stress to plane strain fracture conditions.

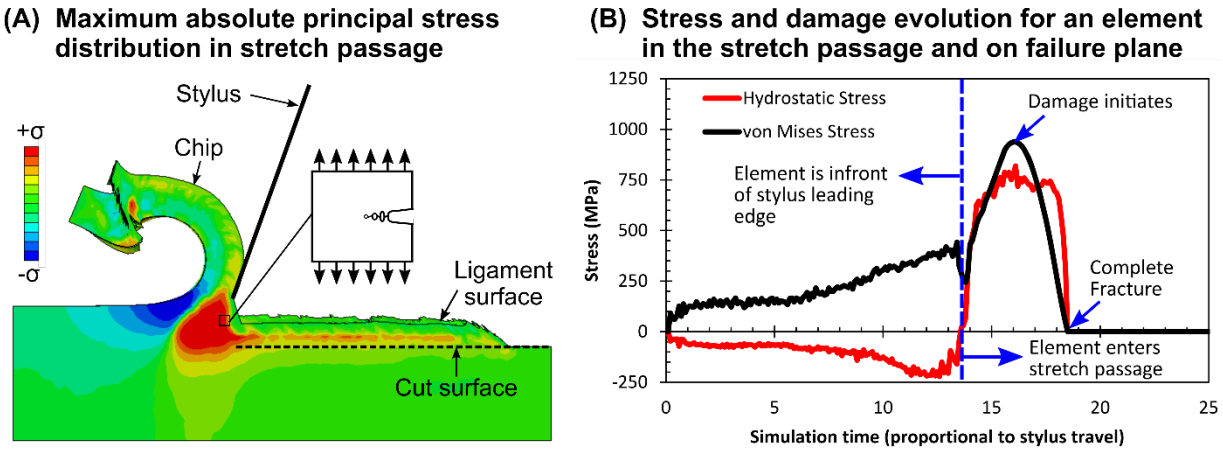

Fig. 9: (A) Maximum absolute principal stress distribution within the substrate. Significant tensile stresses are observed near the crack tip, which is above the cut surface and behind the stylus cutting edge. (B) Evolution of stress state for an element within the material stretch passage as predicted by FEA.

4 Conclusions

Recent advancements in NDE technologies are providing engineers with mechanical property measurements that can be confidently used in lieu of traditional laboratory tests for quality control, condition assessment, and design. This paper summarized progress in using the HSD Tester, a new NDE method for determining yield strength and longitudinal seam characteristics. It also highlighted the NDTT which measures an index of fracture toughness for ductile metals by combining a wedge-shaped stylus with an upstream stretch passage. NDE material verification of transmission pipelines has a great potential to support the assessment of fitness for service, pipeline integrity programs, and life extension of infrastructure.

5 References

[1] Pipeline and Hazardous Materials Safety Administration, "Annual Report Mileage for Natrual Gas Transmission and Gathering Systems," Sep 2017.

[2] ASTM International, "ASTM E10 - Standard Test Method for Brinell Hardness of Metallic Materials," *ASTM E10-17*, 2017.

[3] F.M. Haggag, "In-situ measurements of mechanical properties using novel automated ball indentation systems," *Small Specimen Test Techniques Applied to Nuclear Reactor Vessel Thermal Annealing and Plant Life Extension, ASTM STP 1204*, W. R. Corwin F. M. Haggag, and W. L. Server, Eds., ASTM, Philadelphia, 1993.

[4] M. Dao, K. Chollacoop, K.J. van Vliet, T.A. Venkatesh and S. Suresh, "Computational modeling of the forward and reverse problems in instrumented sharp indentation," *Acta Materialia*, 49, 2001.

[5] N. Chollacoop, M. Dao and S. Suresh, "Depth-sensing instrumented indentation with dual sharp indenters," *Acta Materialia*, 51 2003.

[6] S.C. Bellemare, M. Dao and S. Suresh, "The frictional sliding response of elasto-plastic materials in contact with a conical indenter," *International Journal of Solids and Structures*, 44(6), 2007.
[7] S.C. Bellemare, M. Dao and S. Suresh, "Effects of mechanical properties and surface friction on elasto-plastic sliding contact," *Mechanics of Materials*, 40, 2008.
[8] S.C. Bellemare, M. Dao and S. Suresh, "A new method for evaluating the plastic properties of materials through instrumented frictional sliding tests," *Acta Materialia*, 58, 2010.
[9] ASTM International, "ASTM E8 - Standard Test Method for Tensile Testing of Metallic Materials," 2017.
[10] M.J. Tarkanian, S.D. Palkovic, B.M. Wiley, K. Taniguchi, S.C. Bellemare, "Measurement of mechanical properties of steel pipelines with a portable NDT device," *Aging Pipelines Conference*, 2015.
[11] S.D. Palkovic, K. Taniguchi and S.C. Bellemare, "In-ditch materials verification methods and equipment for steel strength and toughness," *Pipeline Pigging and Integrity Management Conference*, 2017.
[12] Code of Federal Regulations (CFR), "Additional Design Requirements for Steel Pipe using Alternative Maximum Allowable Operating Pressure," *49 CFR 192.112*, 2011.
[13] Abaqus V. 6.14 Documentation. Dassault Systemes Simulia Corporation. 2014.
[14] Hooputra H, Gese H, Dell H, Werner H. A comprehensive failure model for crashworthiness simulation of aluminium extrusions. International Journal of Crashworthiness. 2004;9(5):449-64.